



HAL
open science

Investigating the Reactivity of a Novel Methacrylic Transmer in Solution RAFT-SCVP and Its Impact on the Structure of the Resulting Hyperbranched Polymers

Typhaine Despres, Tiffaine Fabre, Samuel Legeay, Guillaume Bastiat, Franck D'agosto, Muriel Lansalot, Morwenna Pearson-Long, Sandie Piogé, Sagrario Pascual

► To cite this version:

Typhaine Despres, Tiffaine Fabre, Samuel Legeay, Guillaume Bastiat, Franck D'agosto, et al.. Investigating the Reactivity of a Novel Methacrylic Transmer in Solution RAFT-SCVP and Its Impact on the Structure of the Resulting Hyperbranched Polymers. *Macromolecules*, 2024, 57 (5), pp.2421-2431. 10.1021/acs.macromol.3c02498 . hal-04511108

HAL Id: hal-04511108

<https://univ-angers.hal.science/hal-04511108v1>

Submitted on 18 Nov 2024

HAL is a multi-disciplinary open access archive for the deposit and dissemination of scientific research documents, whether they are published or not. The documents may come from teaching and research institutions in France or abroad, or from public or private research centers.

L'archive ouverte pluridisciplinaire **HAL**, est destinée au dépôt et à la diffusion de documents scientifiques de niveau recherche, publiés ou non, émanant des établissements d'enseignement et de recherche français ou étrangers, des laboratoires publics ou privés.

Investigating the Reactivity of a Novel Methacrylic Transmer in Solution RAFT-SCVP and Its Impact on the Structure of the Resulting Hyperbranched Polymers

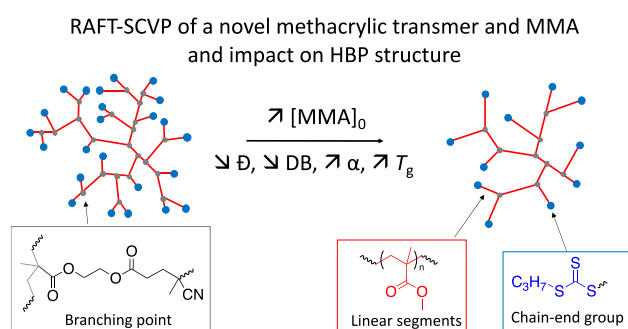
Typhaine Despres,^a Tiffaine Fabre,^b Samuel Legeay,^c Guillaume Bastiat,^c Franck D'Agosto,^b Muriel Lansalot,^b Morwenna Pearson-Long,^a Sandie Piogé,^a Sagrario Pascual*,^a

^a Institut des Molécules et Matériaux du Mans, UMR 6283 CNRS – Le Mans Université, Avenue Olivier Messiaen, 72085 Le Mans Cedex, France

^b Univ Lyon, Université Claude Bernard Lyon 1, CPE Lyon, CNRS, UMR 5128, Catalysis, Polymerization, Processes and Materials (CP2M), 43 Bd du 11 novembre 1918, 69616 Villeurbanne, France

^c Univ Angers, Inserm, CNRS, MINT, SFR ICAT, 49000 Angers, France

FOR TABLE OF CONTENTS USE ONLY



ABSTRACT

A novel methacrylic-based R-transmer, named 2-(methacryloyloxy)ethyl 4-cyano-4-(((propylthio)carbonothioyl)thio)pentanoate, was synthesized and its reactivity (propagation *versus* reversible chain transfer) in reversible addition-fragmentation chain transfer self-condensing vinyl polymerization (RAFT-SCVP) with methyl methacrylate (MMA) was studied to apprehend its impact on hyperbranched polymers (HBP) structure. The resulting HBP were characterized by NMR spectroscopy, SEC and DSC to determine respectively their composition and degree of branching (DB), number-average molecular weight (M_n) and dispersity (D), and glass transition temperature (T_g). Homopolymers of methacrylic-based R-transmer and copolymers with MMA were considered to study the reactivity of the methacrylic-based R-transmer with different initial molar ratios $[MMA]_0/[R\text{-transmer}]_0$ through kinetic studies, and its consequences on HBP macromolecular characteristics and thermal properties. By varying the $[MMA]_0/[R\text{-transmer}]_0$ ratio from 1/1 to 100/1, HBP with increasing M_n (from 6400 to 14900 g.mol⁻¹) and T_g values (from 36.1 to 87.9 °C), decreasing D values (from 4.07 to 1.71) and DB values (from 0.30 to 0.03) were obtained.

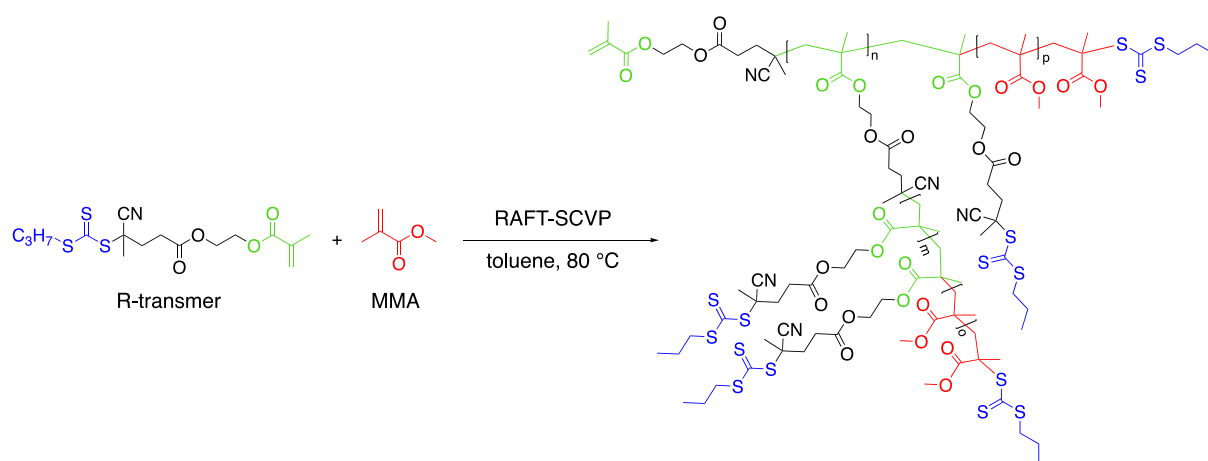
INTRODUCTION

Hyperbranched polymers (HBP) are similar in structure to dendrimers. With their three-dimensional compact structure, they both have large interior volumes and a high number of terminal groups.¹⁻¹² Even if HBP exhibit broader molecular weight distribution than dendrimers, they can be easily synthesized in a one-pot reaction by self-condensing vinyl polymerization (SCVP)¹³ reducing the synthesis cost and time. Recent studies^{14,15} combine the SCVP with reversible-deactivation radical polymerization (RDRP)^{16,17} to produce HBP with narrower molecular weight distribution. This combination takes the benefits from RDRP techniques allowing the synthesis of polymers with well-defined chemical structure,

composition and architecture as inherent irreversible termination and transfer reactions associated to a radical polymerization can be minimized. Limiting chain-transfer or termination reactions also avoids the formation of gel during polymerization.¹⁸ The most studied combinations are atom transfer radical polymerization (ATRP)-SCVP,¹⁹ nitroxide-mediated polymerization (NMP)-SCVP²⁰ and reversible addition-fragmentation chain transfer polymerization (RAFT)-SCVP.²¹

RAFT-SCVP employs a molecule acting as both a reversible chain *transfer* agent (CTA) and a *monomer*. Also called *transmer*, this molecule is a monomer containing as a side group a thiocarbonylthio moiety. HBP are obtained *via* simultaneous propagation of the monomer moiety and reversible chain transfer to the thiocarbonylthio group.²¹ The monomer moiety can be localized either in the so-called R- or Z-group of the CTA, leading to a *transmer* called R-*transmer* or Z-*transmer*, respectively. Depending on the *transmer* employed in the RAFT-SCVP sequence, the HBP structure will be different: the thiocarbonylthio moiety will be located at each branching point when using a Z-*transmer* and at the terminal groups when using a R-*transmer*.²¹ The R-*transmer* approach is of particular interest to target HBP with a high variety of functional terminal groups. Among R-*transmers*, acrylates,²²⁻²⁶⁷ (meth)acrylamides²⁷⁻²⁸ and styrene²⁹⁻³⁵ derivatives have been considered as polymerizable groups. Concerning methacrylate derivatives, dithiobenzoate-based R-*transmers* with a phenyl Z-group have been reported.³⁶⁻³⁹ Trithiocarbonate-based R-*transmers* displaying a methacryloyl moiety and a thioalkyl or a thioaryl Z-group⁴⁰⁻⁴³ have been rarely reported. Most often, HBP structures and properties were discussed, considering that all thiocarbonylthio-moieties of the R-*transmer* create branching points. The present study rather focuses on the reactivity toward simultaneous propagation and reversible chain transfer in RAFT-SCVP of 2-(methacryloyloxy)ethyl 4-cyano-4-(((propylthio)carbonothioyl)thio)pentanoate, a new methacrylic-based R-*transmer*, to understand the structure of the resulting hyperbranched (co)polymers. Its solution RAFT-SCVP

was first studied to target hyperbranched homopolymers (named HBP-R). Hyperbranched copolymers based on methyl methacrylate (MMA) (named HBP-MMA) were also targeted (**Scheme 1**). Kinetic studies have been performed to determine the relative reactivity of the methacryloyl polymerizable group of the R-transmer toward MMA. High-resolution nuclear magnetic resonance (NMR) analyses and size exclusion chromatography (SEC) analyses were carried out to study the reactivity of the thiocarbonylthio moiety of the R-transmer to quantify its ability to form branching points. The impact of the different initial feed ratios of MMA and R-transmer on the macromolecular characteristics including number-average molecular weight (M_n) and dispersity values (\mathcal{D}), degrees of branching (DB) and on the thermal properties of HBP are investigated. Simultaneous propagation of the methacryloyl moiety and reversible chain transfer to the thiocarbonylthio group of the R-transmer, together with its reactivity toward MMA, were particularly taken into account. This work provides rational knowledge and quantification on the percentage of thiocarbonylthio group of a novel methacrylic-based R-transmer that creates branching points thanks to high-resolution NMR spectroscopy. This approach allows a deeper understanding of HBP structures, when most reported studies³⁶⁻⁴² consider that all thiocarbonylthio-moieties of R-transmer create branching points.



Scheme 1. HBP synthesis using RAFT-SCVP of a methacrylic-based R-transmer and MMA

EXPERIMENTAL SECTION

Materials

Methyl methacrylate (MMA, 99 %, Aldrich) was passed through a basic alumina column before polymerization to remove inhibitor. Potassium *tert*-butoxide (*t*-BuOK, 99.9 %), 1-propanethiol (98 %), carbon disulfide (CS₂, 99 %), solid iodine (I₂, 99.8 %), sodium thiosulfate (Na₂S₂O₃, 99 %), 4,4'-azobis (4-cyanopentanoic acid) (ACPA, 98%), *N,N'*-dicyclohexylcarbodiimide (DCC, 99 %), 4-(*N,N*-dimethylamino)pyridine (DMAP, 99 %), 2-hydroxethyl methacrylate (HEMA, 97 %), 2,2'-azobisisobutyronitrile (AIBN, 98 %), magnesium sulfate (MgSO₄), silica gel (60 Å) and anhydrous toluene were purchased from Aldrich and used without purification. Diethyl ether (Et₂O), ethyl acetate (EtOAc), cyclohexane and methanol are technical grade and were purchased from Carlo Erba.

Characterization techniques

¹H NMR, ¹³C NMR, heteronuclear single quantum coherence (HSQC), heteronuclear multiple bond correlation (HMBC) and ¹³C inverse-gated decoupled NMR have been performed using a Bruker AC-500 MHz NMR spectrometer. SEC analyses of crude samples were performed with a SEC system operating in THF eluent at 35 °C fitted with a guard column (PL gel 5 µm guard Agilent, 50*7.5 mm) and two columns (PL gel 5 µm mixed-C Agilent, 300*7.5 mm), a Waters 2414 differential refractometer (DRI) and a Waters 2998 UV-Visible photodiode array detector. The instrument operated at a flow rate of 1.0 mL.min⁻¹. The samples were filtered through a 0.45 µm PTFE filter. The average molecular weights (number-average molecular weight M_n , weight-average molecular weight M_w) and dispersity ($D = M_w / M_n$) values were calculated using Breeze 2 software. Purified polymers were analyzed by SEC using multiple detectors with a SEC system operating in THF eluent at 35 °C fitted with a guard column (PL gel 5 µm) and two columns (PL gel 5 µm mixed-D Agilent, 2*30 cm), and equipped with a multi-angle light scattering (MALS) minidawn TREOS Wyatt detector, a ViscoStar II Wyatt viscometer and a Shimadzu refractive index detector. The instrument operated at a flow

rate of 1.0 mL.min⁻¹. The absolute average molecular weights (M_n and M_w) and dispersity (D) values were calculated using Astra 5 software. The polymer samples were filtered through a 0.22 μ m PTFE filter. Measurements of dn/dc have been performed using an OptiLab rEX from Wyatt Technology Corporation ($\lambda_0 = 632$ nm). The refractive index increment was measured in THF at five various concentrations ranging from 1 to 5 g.L⁻¹. Differential scanning calorimetry (DSC) measurements were performed on a DSC25 using a cooling system RCS120 in aluminium pans under nitrogen. Calibration was made with an indium standard. Samples were heated from -120 °C to 100 °C for HBP-R, from -20 °C to 100 °C for HBP-MMA1, HBP-MMA4 and HBP-MMA10, from -20 °C to 120 °C for HBP-MMA100 and from 0 °C to 120 °C for L-MMA at a heating rate of 10 °C.min⁻¹ and under a static nitrogen atmosphere, followed by cooling down to -120 °C, -20 °C or 0 °C for HBP-R, HBP-MMA and L-MMA respectively, at the same rate after an isotherm at 100 °C or 120 °C during 2 min for HBP and L-MMA respectively. Two cycles of heating and cooling experiments were employed, the second one has been used to determine T_g .

Synthesis of 4-(propylthiocarbonothioylthio)-4-cyanopentanoic acid (named TTC)⁴⁴

To a suspension of potassium *tert*-butoxide (5.0 g, 45 mmol) in anhydrous Et₂O (100 mL) at 0 °C, was added dropwise 1-propanethiol (4.05 mL, 45 mmol) under Argon atmosphere. The mixture was stirred 20 min at 0 °C then carbon disulfide (2.7 mL, 45 mmol) was added dropwise. The suspension was filtered to collect potassium *S*-propyltrithiocarbonate as a solid. Iodine (5.90 g, 23 mmol) was added portion-wise to a suspension of the previously prepared potassium *S*-propyltrithiocarbonate in anhydrous Et₂O (200 mL). The mixture was stirred 2 h at room temperature and the solid potassium iodide was filtered off and washed with Et₂O until the powder became white. The brown filtrate was washed with an aqueous saturated solution of Na₂S₂O₃ (3 x 50 mL) to eliminate excess of iodine. The organic layer was dried over MgSO₄,

filtered and concentrated in vacuo to provide *bis*-(propanesulfanyl thiocarbonyl)disulfide (5.95 g, 86 % yield) as a red oil.

To a solution of *bis*-(propanesulfanylthiocarbonyl)disulfide (5.95 g, 19.7 mmol) in EtOAc (135 mL) was added ACPA (7.88 g, 28.1 mmol). The mixture was heated at reflux for 24 h. After solvent evaporation, the residue was dissolved in Et₂O (30 mL) and washed with deionized water (5 x 50 mL). The organic layer was dried over MgSO₄, filtered and concentrated in vacuo to provide 4-(propylthiocarbonothioylthio)-4-cyanopentanoic acid (10.9 g, quantitative yield) as an orange oil.

¹H NMR (400 MHz, CDCl₃): δ (ppm) 3.33 (t, *J* = 7.2 Hz, 2H, CH₂S), 2.76 – 2.39 (m, 4H, CH₂), 1.88 (s, 3H, CH₃), 1.70 (m, 2H, CH₂CH₃), 1.02 (t, *J* = 7.2 Hz, 3H, CH₂CH₃).

¹³C NMR (100.6 MHz, CDCl₃): δ (ppm) 217.0 (C=S), 207.7 (COOH), 176.9 (C=O), 119.0 (C≡N), 46.4 (C), 38.9 (CH₂S), 33.6 (NCCCH₂), 31.0 (CH₂COO), 24.9 (SCCH₃), 21.4 (CH₂CH₃), 13.5 (CH₂CH₃).

Synthesis of 2-(methacryloyloxy)ethyl 4-cyano-4-(((propylthio)carbonothioyl)thio)pentanoate R-transmer

To a 50 mL round-bottom flask, were successively added TTC (1.50 g, 5.41 mmol), DCC (1.23 g, 5.95 mmol), DMAP (0.07 g, 0.541 mmol), HEMA (0.72 mL, 5.95 mmol) and 20 mL of anhydrous toluene. The mixture was stirred overnight at room temperature under Argon atmosphere. After filtration of the urea by-product, the solvent was removed under vacuum and the residue was purified by chromatography on silica gel (cyclohexane/EtOAc 7:3) to provide R-transmer (1.50 g, 71 % yield) as an orange oil.

¹H NMR (400 MHz, CDCl₃): δ (ppm) 6.05 (m, 1H, C=CH₂), 5.53 (m, 1H, C=CH₂), 4.29 (s, 4H, COOCH₂CH₂OCO), 3.25 (t, *J* = 7.3 Hz, 2H, CH₂S), 2.60-2.33 (m, 4H, CH₂CH₂COO), 1.87 (m, 3H, CH₃), 1.80 (s, 3H, SCCH₃), 1.66 (m, 2H, CH₂CH₃), 0.95 (t, *J* = 7.3 Hz, 3H, CH₂CH₃)

^{13}C NMR (100.6 MHz, CDCl_3): δ (ppm) 216.9 (C=S), 171.1 (C=O), 166.9 (C=O), 135.7 (C=CH₂), 126.0 (C=CH₂), 119.8 (C \equiv N), 62.6 (CH₂OCO), 62.1 (CH₂OCO), 46.2 (C), 39 (CH₂S), 38.7 (CNCCH₂), 33.6 (CH₂OCO), 30.8 (CH₂OCO), 24.7 (SCCH₃), 21.2 (CH₂CH₃), 18.1 (CH₂=CCH₃), 13.3 (CH₂CH₃).

RAFT-SCVP of R-transmer

R-transmer (0.48 g, 1.25 mmol) and AIBN (0.062 g, 0.375 mmol) were dissolved in toluene (5 mL) in a three-neck-round-bottom flask equipped with a condenser. The solution was degassed with Argon flow during 30 min before immersing into an oil bath at 80 °C. Samples were withdrawn at different times to determine R-transmer conversion by ^1H NMR analysis (see **Figure S1** in Supporting Information). The solvent of the final solution was removed in vacuo and the residue was dissolved in THF and precipitated in methanol at 0 °C. The precipitate was dried under vacuum and analyzed by ^1H and inverse-gated decoupled (quantitative) ^{13}C NMR spectroscopies to determine the degree of branching (see **Figures S4 and S5** in Supporting Information) and by SEC with multiple detectors in THF (35 °C) using the measured dn/dc value of 0.133 mL.g⁻¹ to determine the number-average molecular weight and the dispersity and α values.

RAFT-SCVP of R-transmer and MMA

Typical procedure for the synthesis of HBP-MMA1, taken as example. R-transmer (2.92 g, 7.5 mmol), MMA (0.8 mL, 7.5 mmol) and AIBN (0.37 g, 2.25 mmol) were dissolved in toluene (5 mL) in a three-neck-round-bottom flask equipped with a condenser. The solution was degassed with Argon flow during 30 min before immersing into an oil bath at 80 °C. Samples were withdrawn at different times to determine R-transmer and MMA conversions by ^1H NMR analysis. The solvent of the final solution was removed in vacuo and the residue was dissolved in THF and precipitated in methanol at 0 °C. The precipitate was dried under vacuum and analyzed by ^1H NMR spectroscopy to determine the degree of branching and the

experimental MMA/R-transmer molar ratio, and by SEC with multiple detectors in THF (35 °C) using the measured dn/dc value of 0.124 mL.g⁻¹ to determine the number-average molecular weight and the dispersity and α values.

For the four other ratios (HBP-MMA4, HBP-MMA10, HBP-MMA100, HBP-MMA100B), $[MMA]_0 + [R\text{-transmer}]_0 = 3 \text{ mol.L}^{-1}$ was kept constant. The exact quantities of reagents and the measured dn/dc values are reported in **Table S1** in Supplementary Information.

RAFT polymerization of MMA

TTC (0.042 g, 0.15 mmol), MMA (1.72 mL, 14.9 mmol) and AIBN (0.007 g, 0.045 mmol) were dissolved in toluene (5 mL) in a three-neck-round-bottom flask equipped with a condenser. The solution was degassed with Argon flow during 30 min before immersing into an oil bath at 80 °C. Samples were withdrawn at different times to determine MMA conversion by ¹H NMR analysis. The solvent of the final solution was removed in vacuo and the residue was dissolved in THF and precipitated in methanol at 0 °C. The precipitate was dried under vacuum and analyzed by ¹H NMR spectroscopy and by SEC with multiple detectors in THF (35 °C) using dn/dc value to determine the number-average molecular weight and the dispersity and α values.

RESULTS AND DISCUSSION

Synthesis of hyperbranched homopolymers (HBP-R) by RAFT-SCVP of the methacrylic-based R-transmer

A new methacrylic-based R-transmer, the 2-(methacryloyloxy)ethyl 4-cyano-4-(((propylthio)carbonothioyl)thio)pentanoate was synthesized through the esterification of 4-(propylthiocarbonothioylthio)-4-cyanopentanoic acid (TTC)⁴⁴ and 2-hydroxyethyl methacrylate (HEMA) in toluene at room temperature. It was successfully synthesized in 71 % yield after purification.

The RAFT-SCVP of the methacrylic-based R-transmer was performed in toluene ($[R\text{-transmer}]_0 = 1.25 \text{ mol.L}^{-1}$) at $80 \text{ }^\circ\text{C}$ using 2,2'-azobisisobutyronitrile (AIBN) as initiator and an initial molar ratio of $[R\text{-transmer}]_0/[AIBN]_0$ equal to 1/0.3. Samples were withdrawn from the reaction medium at different times. The R-transmer conversion was calculated *via* proton NMR ($^1\text{H NMR}$) analysis of withdrawn samples by comparing the integration of the vinylic proton signals between 5.61 and 6.14 ppm with the one of toluene methyl group at 2.35 ppm, used as internal reference (see **Figure S1** and **Equation S1** in Supporting Information). **Figure 1** shows the evolution of R-transmer conversion and $\ln([M]_0/[M]_t)$ with time. After a short inhibition period, a first order kinetic was observed for the R-transmer consumption reaction. This behavior is consistent with a constant concentration of propagating radicals after the inhibition period.

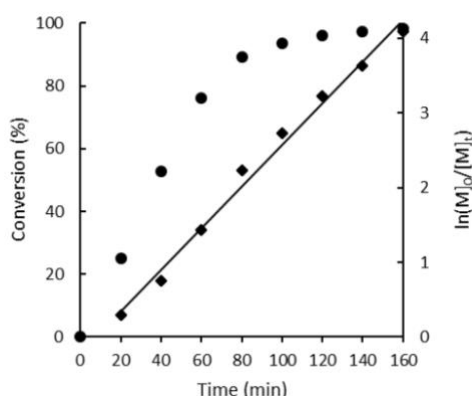


Figure 1. R-transmer conversion (●) and $\ln([M]_0/[M]_t)$ (■) as function of time for the RAFT-SCVP of R-transmer in toluene at $80 \text{ }^\circ\text{C}$ using $[R\text{-transmer}]_0/[AIBN]_0 = 1/0.3$ ($[R\text{-transmer}]_0 = 1.25 \text{ mol.L}^{-1}$)

The M_n from crude samples were determined by SEC analysis (**Figure 2**). A shift of SEC traces toward lower retention times is observed and the signal of R-transmer at 18.5 mL decreases when the reaction time increases. This is compatible with an increase of the average molecular weight of the HBP with R-transmer conversion as reaction time increases. Moreover,

the chromatograms of crude mixtures withdrawn at different times show a non-gaussian profile, reflecting an hyperbranched structure.³⁶

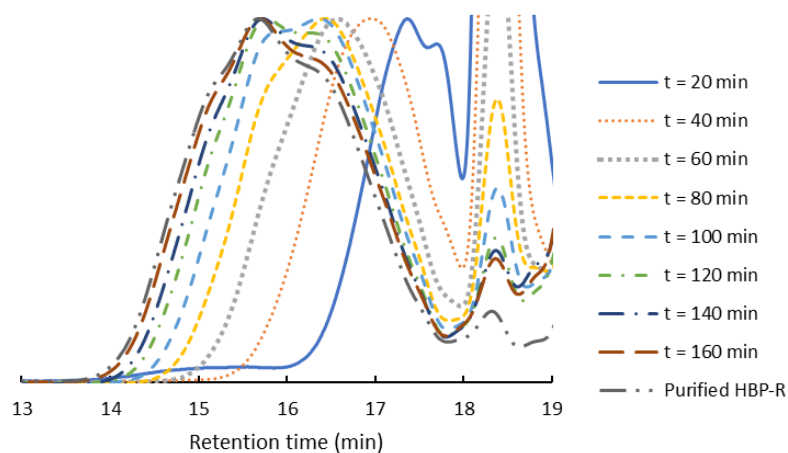


Figure 2. Overlaid of SEC traces of the reaction medium at different times during the RAFT-SCVP of R-transmer in toluene at 80 °C using $[R\text{-transmer}]_0/[AIBN]_0 = 1/0.3$ ($[R\text{-transmer}]_0 = 1.25 \text{ mol.L}^{-1}$) and of the purified HBP-R

After 160 min of reaction, the HBP-R obtained with a quantitative R-transmer conversion was purified by precipitation in cold methanol and dried under vacuum. Characterizations by carbon (¹³C) quantitative NMR, differential scanning calorimetry (DSC) and SEC with multiple detectors including multi-angle light scattering (MALS) and viscosimetry were performed to determine the DB, the glass transition temperature (T_g), the M_n and D values as well as the Mark-Houwink-Sakurada (MHS) coefficient (α) of final HBP. The α value determined from the slope of the MHS plot ($\log([\eta])$ versus $\log(M_v)$, with M_v the viscosimetric molecular weight) corresponds to the polymer conformation in solution: a value between 0.5 and 1.0 reveals a randomly coiled linear polymer and a value lower than 0.5 suggests a spherical shape hyperbranched polymer.³

Table 1 summarizes the polymerization results. The HBP-R has a M_n equal to 3200 g.mol⁻¹ and a D value of 4.46 by SEC with MALS detection using a measured dn/dc value of 0.133 mL.g⁻¹. The MHS plot shows two slopes (see **Figure S2** in Supporting Information) indicating two α values. A first slope at the lowest M_v (between 2.8 and 3.5 for $\log(M_v)$) with an α value equals to 0.11. The second slope at high M_v (between 3.6 and 4.5 for $\log(M_v)$) corresponds to

an α value of 0.30. This set of values is consistent with the formation of HBP and is also in accordance with the multimodal size exclusion chromatograms, indicating the presence of, at least, two different hyperbranched polymer structures, with the one of lower molecular weights having higher branching points as the MHS coefficient α is lower. This result is compatible with a sequential reactivity of the R-transmer toward propagation of the methacryloyl moiety and reversible chain transfer to the trithiocarbonate of R-transmer with time. Therefore, it appears that lightly branched polymers are formed at the beginning of the polymerization whereas highly branched polymers are formed at the end of the polymerization.

The DB value of the HBP-R (see structure **Figure S3** in Supporting Information) after purification has been determined according to the method described by Gao's group^{45,46} using quantitative ¹³C NMR analyses *via* an inverse-gated decoupled ¹³C NMR sequence and with the help of 2D NMR correlations to precisely assign each signal (see **Equations S2-S5, Figures S4 and S5** in Supporting Information). For the RAFT-SCVP of R-transmer using $[R\text{-transmer}]_0/[AIBN]_0 = 1/0.3$, the DB value obtained is 0.50 corresponding to an hyperbranched structure. The DB can also be determined by ¹H NMR analysis method described by Zhang *et al.*²⁹ The experimental DB is the inverse of the number of repeating units per branch (RB) which is determined by ¹H NMR analysis (**Figure 3**) by comparing overall repeating units to branching units. Overall repeating units are characterized by R-transmer units (CH₂-CH₂-O-C=O signal at 4.30 ppm, H₁ in **Figure 3**). The branching units are defined by the difference between R-transmer units (CH₂-CH₂-O-C=O signal at 4.30 ppm, H₁ in **Figure 3**) and the trithiocarbonate moieties that did not react (S-CH₂ signal at 3.21 ppm, H_{2'} in **Figure 3**)⁴³ (see **Equations S6 and S7** in Supporting Information). An experimental DB value of 0.77 is obtained. This difference in DB values calculated by both methods can be explained by an underestimation of integration in quantitative ¹³C NMR. Therefore, the ¹H NMR analysis method is preferred.

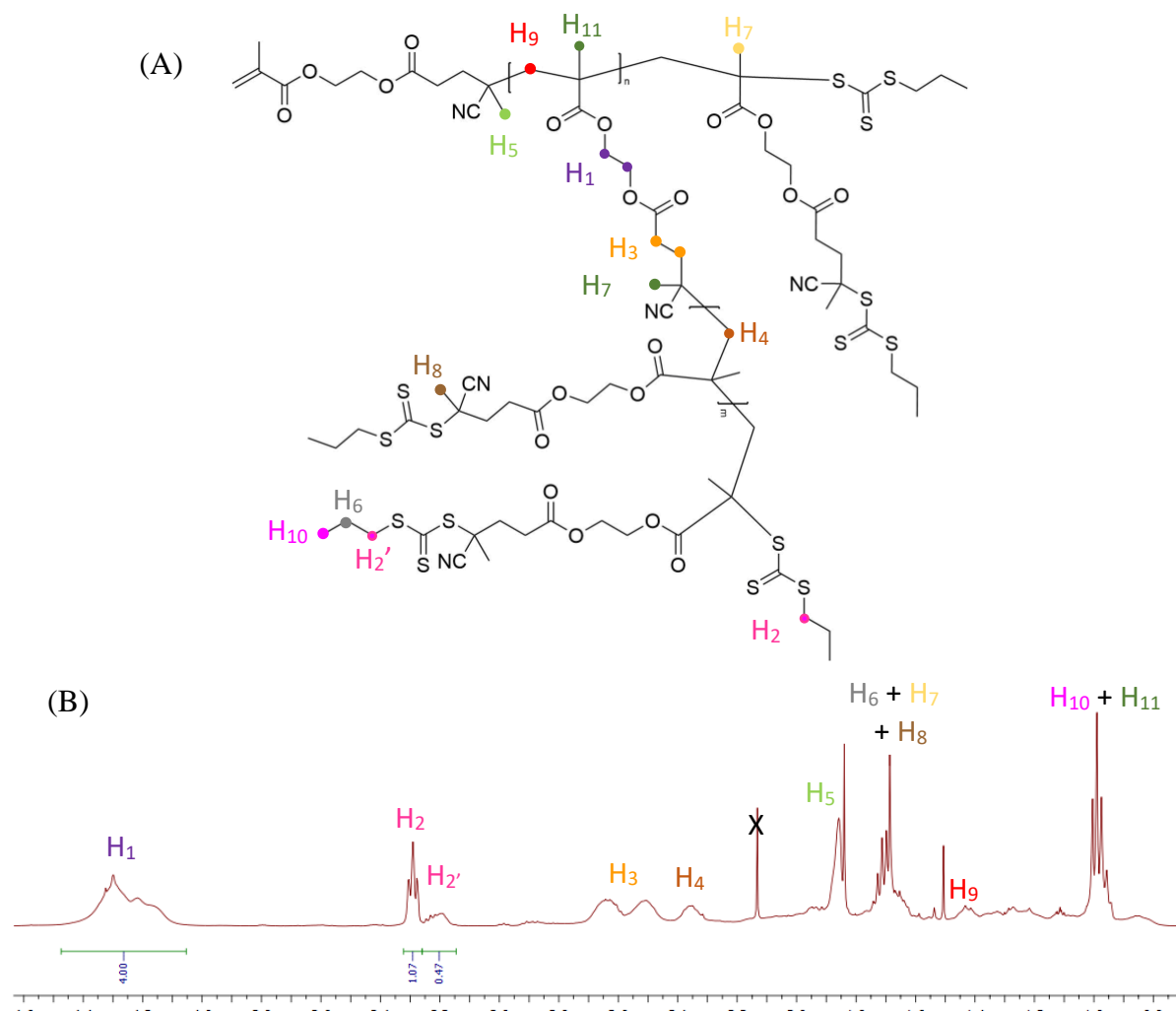


Figure 3. (A) Representative structure of purified HBP-R and (B) ¹H NMR spectrum of purified HBP-R obtained by RAFT-SCVP of R-transmer in toluene at 80 °C using $[R\text{-transmer}]_0/[AIBN]_0 = 1/0.3$ ($[R\text{-transmer}]_0 = 1.25 \text{ mol.L}^{-1}$)

The thermal analysis of the purified HBP-R was then studied by DSC analysis carried out between -120 °C and 100 °C. A T_g value of -0.7 °C was observed (see **Figure S6** in Supporting Information). This low T_g could be explained by a high number of chain ends compatible with a high DB that would enhance free volumes.

Synthesis of hyperbranched copolymers by RAFT-SCVP of the methacrylic-based R-transmer and MMA

RAFT-SCVP of the R-transmer and MMA were performed in toluene, and the impact of the $[MMA]_0/[R\text{-transmer}]_0$ ratios on the macromolecular characteristics (M_n and \bar{D}), on the

structural characteristics (DB) and on the thermal properties (T_g) of the resulting HBP was studied.

A first RAFT-SCVP of R-transmer with MMA was carried out in toluene ($[R\text{-transmer}]_0 + [MMA]_0 = 3 \text{ mol.L}^{-1}$) at 80 °C using AIBN as initiator with a molar ratio of $[MMA]_0/[R\text{-transmer}]_0/[AIBN]_0$ equal to 1/1/0.3. The R-transmer and MMA conversions were determined by ^1H NMR spectroscopy using toluene as internal standard (see **Figure S7** in Supporting Information). The results are shown in **Table 1**. **Figure 4** shows first order kinetics for both R-transmer and MMA consumption reactions after an inhibition period (ca. 20 min). The consumption rate of R-transmer is slightly higher than that of MMA. High R-transmer and MMA conversions (98 and 96 %, respectively) were achieved in 100 min (**Table 1** and **Figure 4**).

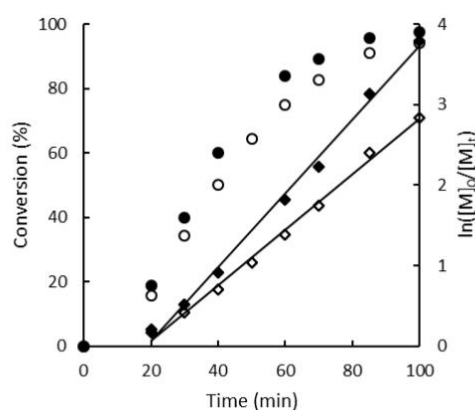


Figure 4. R-transmer (●) and MMA (○) conversions and $\ln([M]_0/[M]_t)$ for R-transmer (■) and for MMA (□) as function of time for the RAFT-SCVP of R-transmer and MMA in toluene at 80 °C using $[MMA]_0/[R\text{-transmer}]_0/[AIBN]_0 = 1/1/0.3$ ($[R\text{-transmer}]_0 + [MMA]_0 = 3 \text{ mol.L}^{-1}$)

SEC analyses have been performed on crude mixtures withdrawn from the reaction medium at different times. The chromatograms obtained (**Figure 5A**) show a shift towards lower retention times and a multimodality increases with reaction time. At 20 min, the α value determined from the slope of the MHS plot of withdrawn sample is equal to 0.58 whereas it is equal to 0.35 at final time. First steps of polymerization are characterized by lightly branched polymers due to the consumption of methacryloyl moieties of R-transmer and MMA driving

linear segments. Then, after consumption of most methacryloyl groups and MMA, there is an increase of the ratio of branching points in comparison with linear segments. After 100 min of reaction, the raw sample was precipitated and the SEC trace of the purified HBP-MMA1 shows a removal of the lower molecular weights macromolecular chains due to the fractionation. The resulting HBP-MMA1 has a M_n equal to $6500 \text{ g}\cdot\text{mol}^{-1}$ and a D value of 3.60 *via* SEC-MALS using the measured dn/dc value equal to $0.124 \text{ mL}\cdot\text{g}^{-1}$ (**Table 1**).

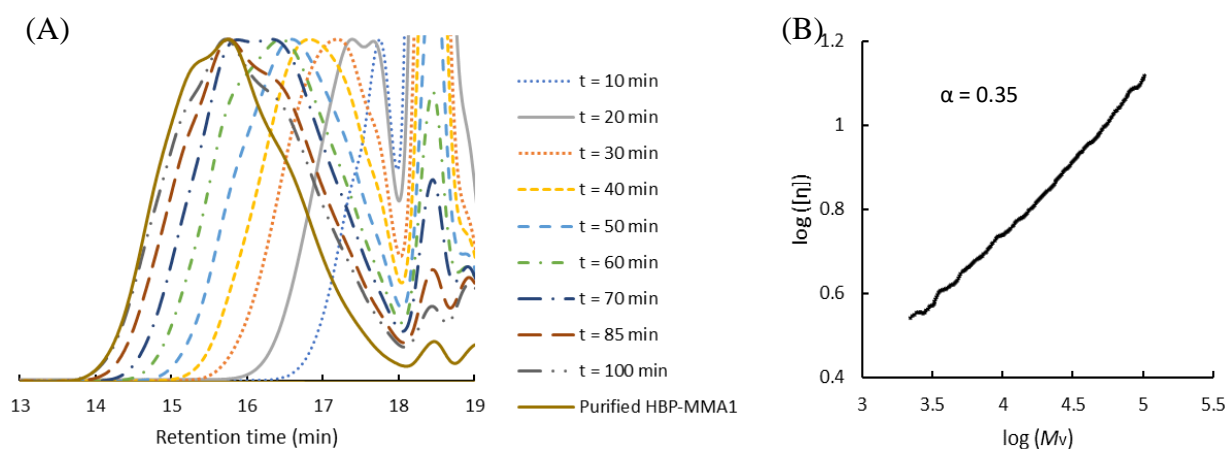


Figure 5. (A) Overlaid of SEC chromatograms of the crude reaction medium at different times and of purified HBP-MMA1 (B) Mark-Houwink-Sakurada plot for the purified HBP-MMA1 obtained from RAFT-SCVP of R-transmer and MMA in toluene at $80 \text{ }^\circ\text{C}$ using $[\text{MMA}]_0/[\text{R-transmer}]_0/[\text{AIBN}]_0 = 1/1/0.3$ obtained by SEC using viscosimetric detection ($T = 35 \text{ }^\circ\text{C}$)

The composition of the purified (HBP-MMA1 copolymer) was determined by ^1H NMR spectroscopy by comparing integration of OCH_3 signal (labelled H_2 in **Figure 6**) at 3.62 ppm characteristic of MMA units, with the integration of $\text{CH}_2\text{-CH}_2\text{-O-C=O}$ signal (labelled H_1 in **Figure 6**) at 4.29 ppm characteristic of R-transmer units (see **Equation S8** in Supporting Information). The final MMA/R-transmer molar ratio obtained for HBP-MMA1 is equal to 1.1/1. This value is in relative good agreement with the initial ratio ($[\text{MMA}]_0/[\text{R-transmer}]_0 = 1/1$).

The α value determined from the slope of the MHS plot (**Figure 5B**) was equal to 0.35 (**Table 1**). This value is higher than the one obtained for the HBP-R, which means, as could be expected, a lower fraction of branching points for the HBP-MMA1 copolymer.

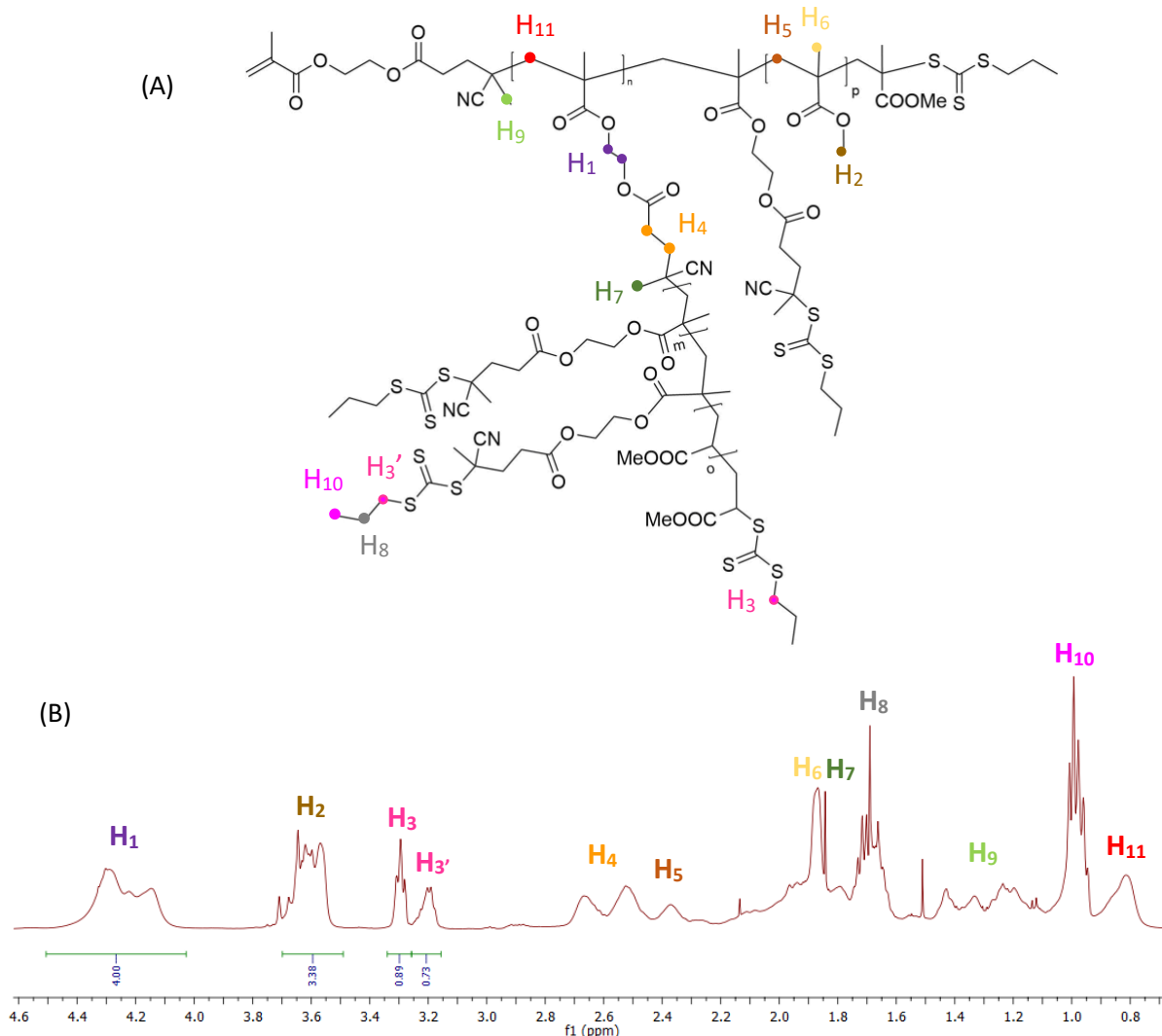


Figure 6. (A) Representative structure of purified HBP-MMA1 and (B) ¹H NMR spectrum of purified HBP-MMA1 obtained by RAFT-SCVP of R-transmer and MMA in toluene at 80 °C using [MMA]₀/[R-transmer]₀/[AIBN]₀ = 1/1/0.3 ([R-transmer]₀ + [MMA]₀ = 3 mol.L⁻¹)

The DB of HBP-MMA1 was determined by ¹H NMR analysis. Overall repeating units are characterized by MMA units (O-CH₃ signal at 3.62 ppm, H₂ in **Figure 6**) and R-transmer units (CH₂-CH₂-O-C=O signal at 4.29 ppm, H₁ in **Figure 6**). The branching units are defined by the difference between R-transmer units (CH₂-CH₂-O-C=O signal at 4.29 ppm, H₁ **Figure 6**) and the trithiocarbonate moieties that did not react (S-CH₂ signal at 3.20 ppm, H₃' in **Figure 6**)⁴³

(see **Equations S7** and **S9** in Supporting Information). An experimental DB value of 0.30 is obtained. This value is lower than the theoretical DB of 0.49 (**Table 1**), which depends on the MMA/R-transmer molar ratio. The difference between experimental and theoretical DB values can be explained by the approximation in the theoretical equation, which considers that all R-transmer units create branching points. Experimentally, it has been determined that 55 % of trithiocarbonate moieties create a branching point by comparing the integration values of S-CH₂ signals at 3.22 ppm (unreacted trithiocarbonate moieties, H₃' in **Figure 6**) and at 3.32 ppm (reacted trithiocarbonate moieties, H₃ in **Figure 6**).

DSC analysis was performed between -20 °C and 100 °C and showed a T_g of 36.1 °C for HBP-MMA1 (**Figure 9D**). This unique T_g features a homogeneous structure of the HBP-MMA1 obtained from RAFT-SCVP. To compare the thermal properties of the HBP structure to a linear polymer, a RAFT polymerization of MMA using 4-(propylthiocarbonothioylthio)-4-cyanopentanoic acid (TTC) as CTA, precursor of the R-transmer used in this study, has been performed (L-MMA100B, **Table 1**). After purification, the linear L-MMA100B with a similar range of molecular weights and a lower D value (**Table 1**) was analyzed by DSC as it has been reported that T_g was not influenced by the molecular weight distribution.⁴⁷ A higher T_g , for L-MMA100B (equal to 73.9 °C) in comparison with HBP-MMA1 was obtained (**Table 1**). The presence of the R-transmer units in HBP-MMA1 increases the number of chain-ends leading to a lower T_g for HBP structure in comparison with the linear one.

RAFT-SCVP was then performed using other initial molar ratios of $[MMA]_0/[R\text{-transmer}]_0$ (= 100/1, 10/1 and 4/1, called HBP-MMA100, HBP-MMA10 and HBP-MMA4 in **Table 1**, respectively) with the aim of studying the impact of this ratio on the structural characteristics and thermal properties of the HBP obtained. In this study, the $[MMA]_0 + [R\text{-transmer}]_0$ (= 3 mol.L⁻¹) concentration and the ratio $[R\text{-transmer}]_0/[AIBN]_0$ (= 1/0.3) were kept constant.

For the three lowest ratios $[MMA]_0/[R\text{-transmer}]_0$ (1/1 for HBP-MMA1, 4/1 for HBP-MMA4 and 10/1 for HBP-MMA10), after a slight inhibition period, high conversions were reached for both MMA and R-transmer after respectively 1h40, 2h40 and 9 h (**Figure 7A**, **Figure S8** and **Table 1**). For the highest ratio $[MMA]_0/[R\text{-transmer}]_0$ (100/1 for HBP-MMA100, **Figure 7A**, **Figure S8** and **Table 1**), R-transmer conversion could not be determined as the signals corresponding to the R-transmer vinylic protons are hidden in background noise. However, 83 % MMA conversion was reached only after 24 h of reaction. To confirm this maximal conversion obtained for HBP-MMA100, a RAFT polymerization of MMA using TTC with a similar ratio ($[MMA]_0/[TTC]_0/[AIBN]_0 = 100/1/0.3$) was performed (L-MMA100, **Table 1**). The same plateau was observed with a maximum conversion of 84 % reached after 24 h with a similar slow kinetics (see **Figure S9** in Supporting Information). This is probably due to the lower quantity of AIBN in the reaction medium for the synthesis of HBP-MMA100 (0.045 mmol) in comparison with the one used for HBP-MMA10 (0.41 mmol) for instance. Indeed, the impact of $[AIBN]_0$ on kinetics is highlighted by comparing RAFT-SCVP of MMA and R-transmer by increasing the AIBN quantity while keeping the same $[MMA]_0/[R\text{-transmer}]_0$ ratio: $[MMA]_0/[R\text{-transmer}]_0/[AIBN]_0 = 100/1/15.1$ for HBP-MMA100B and $[MMA]_0/[R\text{-transmer}]_0/[AIBN]_0 = 100/1/0.3$ for HBP-MMA100. A faster kinetic is observed for the highest AIBN quantity, which is consistent with a higher concentration of radicals in the reaction medium (**Figure 7B** and **Table 1**).

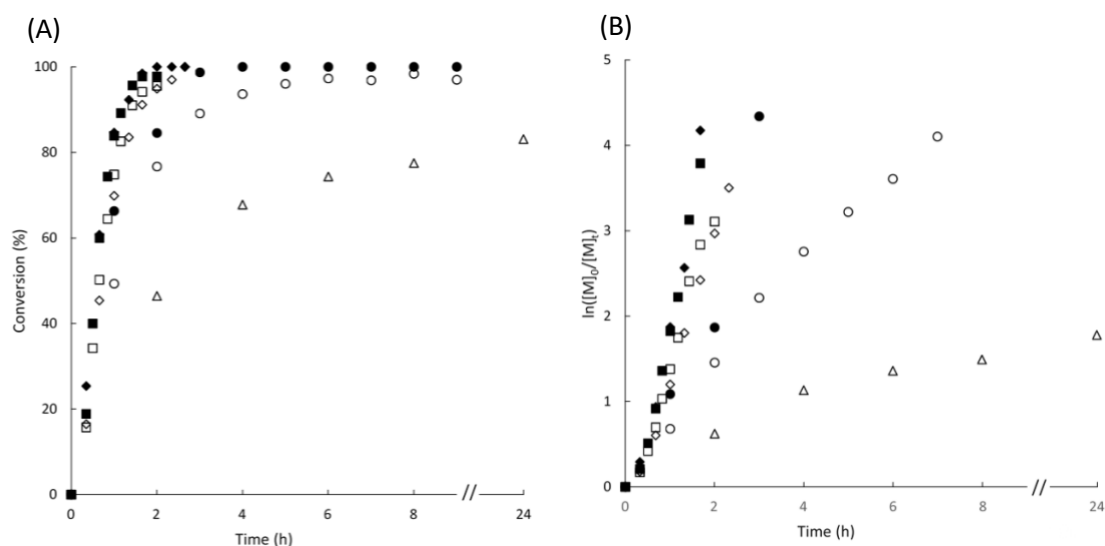


Figure 7. R-transmer (filled symbols) and MMA (empty symbols) conversions (A) and $\ln([M]_0/[M]_t)$ (B) as function of time for the HBP-MMA copolymers synthesized by the RAFT-SCVP of R-transmer and MMA in toluene at 80 °C with $[R\text{-transmer}]_0 + [MMA]_0 = 3 \text{ mol.L}^{-1}$. $[MMA]_0/[R\text{-transmer}]_0/[AIBN]_0 = 100/1/0.3$ (HBP-MMA100) (Δ); 10/1/0.3 (HBP-MMA10) (\bullet, \circ); 4/1/0.3 (HBP-MMA4) (\blacklozenge, \diamond); 1/1/0.3 (HBP-MMA1) (\blacksquare, \square); 100/1/15.1 (HBP-MMA100B) (\times). Zooms between $t = 0$ and $t = 3$ h are shown in Figure S8 in Supporting Information.

The overlaid of SEC traces of the crude mixture samples withdrawn from the reaction medium at different times are shown in **Figure 8** for the different initial molar ratios $[MMA]_0/[R\text{-transmer}]_0$. For all, a shift of the molecular weight distributions toward lower retention times is observed when the reaction time increases, meaning that M_n increase with time and conversion. It appears that chromatograms with several populations are more prominent as $[MMA]_0/[R\text{-transmer}]_0$ ratio decreases (**Figure 8**). This observation is consistent with the increase of R-transmer quantity leading to SEC traces of HBP-MMA which shape is closer to that of the HBP-R. As for HBP-MMA1, a fractionation occurs during the precipitation of raw samples as shown by the removal of lower molecular weights macromolecules (**Figure 8**).

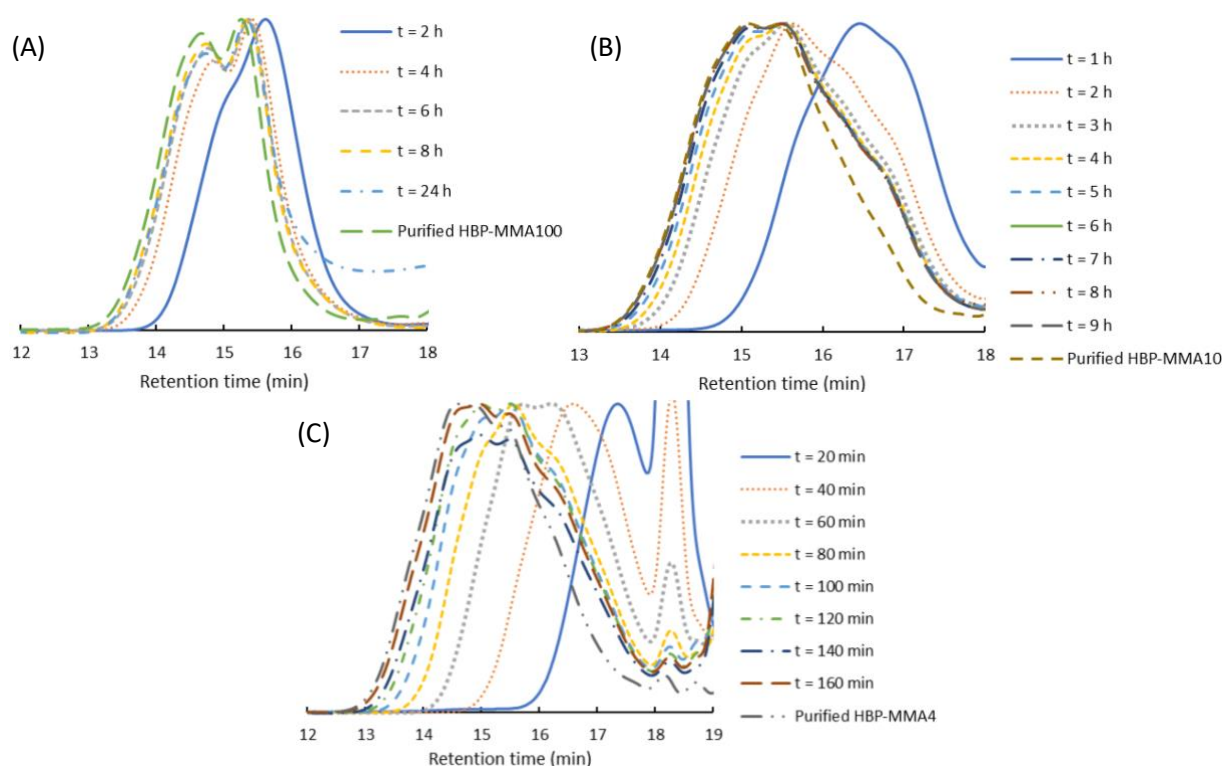


Figure 8. Overlaid of SEC traces of the reaction medium at different times and of purified HBP-MMA copolymers synthesized by the RAFT-SCVP of R-transmer and MMA in toluene at 80 °C with $[R\text{-transmer}]_0 + [MMA]_0 = 3 \text{ mol.L}^{-1}$. $[MMA]_0/[R\text{-transmer}]_0/[AIBN]_0 = 100/1/0.3$ (HBP-MMA100) (A); 10/1/0.3 (HBP-MMA10) (B); 4/1/0.3 (HBP-MMA4) (C)

For the purified HBP-MMA copolymers, experimental MMA/R-transmer molar ratios determined by ^1H NMR fitted well with initial ratios with respectively 87.5/1, 12.1/1, 4.3/1 and 1.1/1 for $[MMA]_0/[R\text{-transmer}]_0 = 100/1$; 10/1 ; 4/1 and 1/1 (**Table 1**).

MHS plots to evaluate the branching rate of purified HBP-MMA (**Figure 9C**) show α values fluctuating between 0.35 (HBP-MMA1) to 0.45 (HBP-MMA100), which confirm the branched structure of these HBP.

As the ratio $[MMA]_0/[R\text{-transmer}]_0$ increases, the DB value decreases (**Table 1**). Thus, the number of repeating units per branch increases, which is consistent with a higher number of MMA units per chain and therefore a higher fraction of linear segments. Even if the evolution of experimental DB agrees with the evolution of the theoretical ones, none of their values are in correlation with the theoretical ones as it seems that all R-transmer does not create branching points. To confirm this hypothesis, further ^1H NMR analyses have been performed. The ratio

of trithiocarbonate moieties that react to create branching points are: 18 %, 31 %, 55 % and 69 % for HBP-MMA10, HBP-MMA4, HBP-MMA1 and HBP-R, respectively. This ratio increases with the increase of R-transmer quantity. Thus, experimental DB gets closer to theoretical one for the HBP with the highest R-transmer quantity.

The T_g values of the HBP increase from 36.1 °C, 45.4 °C, 64.7 °C to 87.9 °C when $[MMA]_0/[R\text{-transmer}]_0$ increases from 1/1 ; 4/1 ; 10/1 to 100/1, respectively. This is probably due to a decrease of free volume as the number of chain ends decreases when $[MMA]_0$ increases. T_g of HBP-MMA100 is equivalent to its linear analogous L-MMA100 (T_g of 88.2°C), an indirect proof of the very likely low DB of this copolymer.

Table 1. Experimental conditions of the RAFT-SCVP of R-transmer with or without MMA and the RAFT polymerization of MMA using AIBN as initiator in toluene at 80 °C. Characteristics of resulting HBP and linear PMMA

Polymer	Chain transfer agent entity	[MMA] ₀ /[R-transmer or [TTC] ₀]/[AIBN] ₀ ^a	Time	Conv. ^b (%)	MMA/R-transmer molar ratio ^c	<i>M</i> _{n,SEC} ^e (g.mol ⁻¹)	<i>D</i> ^e	dn/dc (mL.g ⁻¹) ^f	DB _{th} ^g	DB	α ^j	<i>T</i> _g (°C) ^k
HBP-R	R-transmer	-1/0.3	2h40 min	100	ND ^d	3200	4.46	0.133	ND ^d	0.50 ^h 0.77 ⁱ	0.11 0.30	- 0.7
HBP-MMA1	R-transmer	1/1/0.3	1h40 min	> 96	1.1/1	6500	3.60	0.124	0.49	0.30 ⁱ	0.35	36.1
HBP-MMA4	R-transmer	4/1/0.3	2h40 min	100	4.3/1	9300	4.07	0.110	0.32	0.10 ⁱ	0.34	45.5
HBP-MMA10	R-transmer	10/1/0.3	9 h	100	12.1/1	6400	3.47	0.102	0.17	0.03 ⁱ	0.34	64.7
HBP-MMA100	R-transmer	100/1/0.3	24 h	83*	87.5/1	14900	1.71	0.099	0.02	ND ^d	0.45	87.9
HBP-MMA100B	R-transmer	100/1/15.1	1h30 min	100*	111.1/1	7200	1.50	ND ^d	0.02	ND ^d	0.46	85.0
L-MMA100B	TTC	100/1/0.3	2h20 min	30	ND ^d	4500	1.02	ND ^d	ND ^d	ND ^d	0.57	73.9
L-MMA100	TTC	100/1/0.3	24 h	84	ND ^d	9500	1.11	ND ^d	ND ^d	ND ^d	0.55	88.2

^a [MMA]₀ + [R-transmer]₀ (= 3 mol.L⁻¹) concentration constant, variation of MMA, R-transmer and AIBN number of moles; ^b R-transmer and/or MMA conversions determined by ¹H NMR spectroscopy (*MMA conversion only, R-transmer conversion could not be determined as the signals corresponding to the R-transmer vinylic protons are hidden in background noise); ^c Molar ratio determined by ¹H NMR after purification of HBP; ^d Not determined; ^e Number-average molecular weight and dispersity values determined by SEC with THF as eluent and using multiple detectors; ^f dn/dc value obtained by refractive index measurement; ^g DB_{th} = (2 (1-e^{-(γ+1)})(γ+e^{-(γ+1)})) / (γ+1)² with γ = [MMA]₀/[R-transmer]₀⁴⁸; ^h Degree of branching determined by inverse-gated decoupled (quantitative) ¹³C NMR spectroscopy; ⁱ Degree of branching determined by ¹H NMR spectroscopy; ^j Mark-Houwink-Sakurada coefficient obtained by SEC with multiple detectors using viscosimetry; ^k Glass transition temperature determined by DSC analysis (10 °C.min⁻¹).

The addition of a monomer, here MMA, to the R-transmer polymerization undoubtedly plays an important role on the macromolecular characteristics, structural characteristics and thermal properties of the final HBP (**Table 1**). Indeed, in comparison with HBP-R, HBP-MMA show higher number-average molecular weights for lower dispersities with a delayed apparition of multimodal distributions on SEC traces (**Figure 9A** and **Figure 9B**). For HBP-R and for HBP-MMA, dispersity values increase with conversion as reaching high conversion may lead to a high probability of chain-breaking reactions. The DB and α values obtained for HBP-R and those for HBP-MMA are far apart and lower fractions of branching points are observed for HBP copolymers (**Figure 9C**). These differences in structural characteristics are due to the presence of linear segments which offer a better control on the HBP macromolecular characteristics. A huge difference is also observed for the T_g values (**Figure 9D**) of the HBP copolymers (HBP-MMA), which stand between those of the linear PMMA (L-MMA) and of the HBP homopolymer (HBP-R).

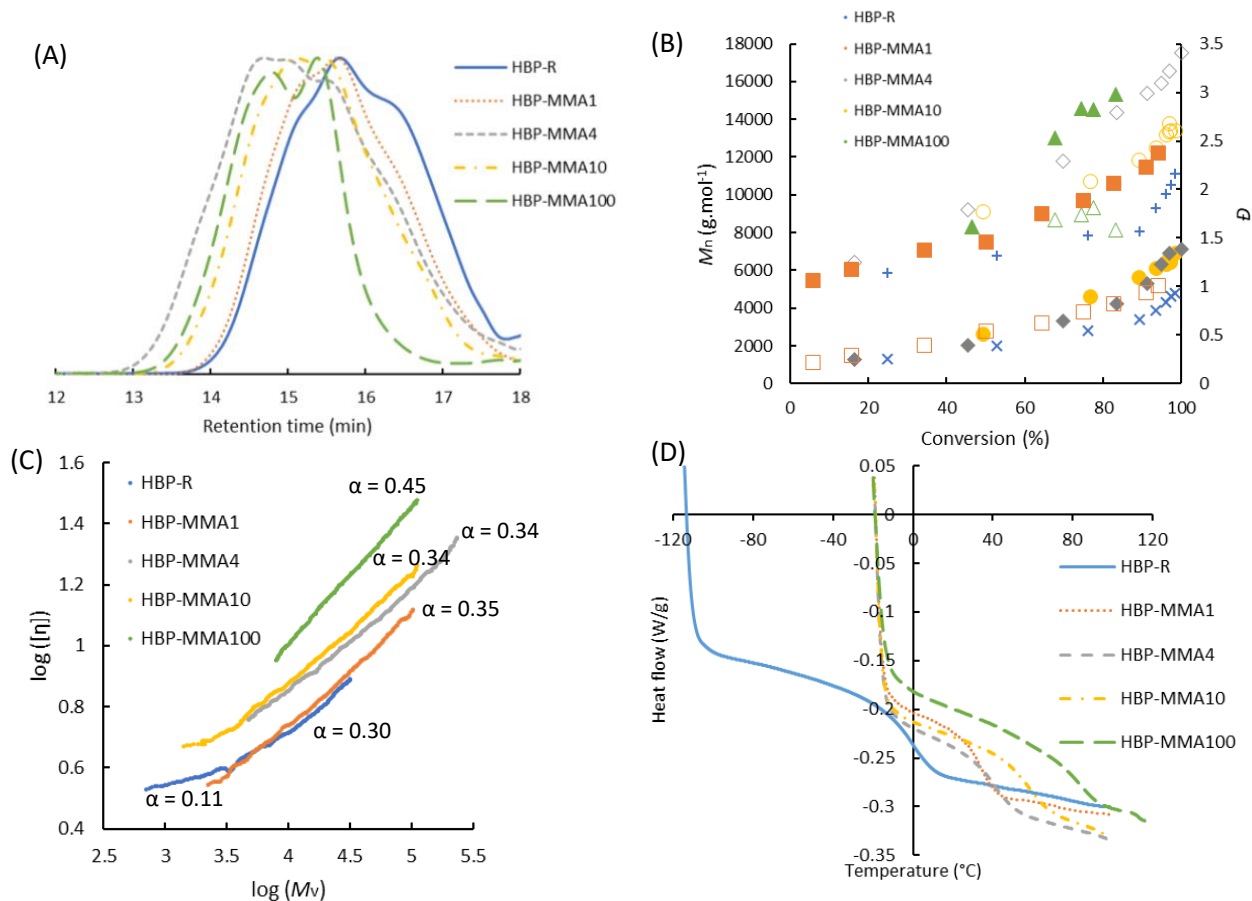


Figure 9. Overlaid of (A) SEC traces; (B) M_n (filled symbols) and \bar{D} (empty symbols) as function of conversion (HBP-R ($\times, +$); HBP-MMA1 (\blacksquare, \square); HBP-MMA4 (\blacklozenge, \diamond); HBP-MMA10 (\bullet, \circ) and HBP-MMA100 ($\blacktriangle, \triangle$)); (C) MHS plots obtained by SEC using viscosimetric detection ($T = 35^\circ\text{C}$) and (D) DSC analyses, for the HBP-R, HBP-MMA1, HBP-MMA4, HBP-MMA10 and HBP-MMA100

CONCLUSION

This paper reports the synthesis of hyperbranched polymers *via* RAFT-SCVP using a novel methacrylic-based R-transmer, the 2-(methacryloyloxy)ethyl 4-cyano-4-(((propylthio) carbonothioyl) thio)pentanoate and the characterization of their molecular structures through kinetics and a range of analytical techniques able to highlight the R-transmer reactivity considering simultaneous propagation and reversible chain transfer. Hyperbranched polymers were prepared using such R-transmer first in homopolymerization, then in copolymerization with MMA with various molar compositions. The addition of MMA to the R-transmer polymerization undoubtedly plays an important role on the macromolecular and structural

characteristics, as well as on the thermal properties of the final HBP. The addition of a MMA monomer gives access to HBP with a better control than with homopolymerization ($\bar{D} = 1.71$ for HBP-MMA100 and $\bar{D} = 4.46$ for HBP-R). An increase of $[\text{MMA}]_0/[\text{R-transmer}]_0$ molar ratio leads to a decrease of branching points and \bar{D} . In contrast, an increase of T_g values is observed with the increase of $[\text{MMA}]_0/[\text{R-transmer}]_0$ molar ratio. This study features a convenient access to HBP with various structures.

REFERENCES

- (1) Malmström, E.; Hult, A. Hyperbranched Polymers: A Review. *Polym. Rev.*, **1997**, *37*, 555-579. DOI: 10.1080/15321799708018375
- (2) Hult, A.; Johansson, M.; Malmström, E. Hyperbranched Polymers. *Advances in Polymer Science*, **1999**, *143*, 1-34. DOI: 10.1007/3-540-49780-3_1
- (3) Jikei, M.; Kakimoto, M. Hyperbranched polymers; a promising new class of materials. *Prog. Polym. Sci.*, **2001**, *26*, 1233-1285. DOI: 10.1016/S0079-6700(01)00018-1
- (4) Aulenta, F.; Hayes, W.; Rannard, S. Dendrimers: a new class of nanoscopic containers and delivery devices. *Eur. Polym. J.*, **2003**, *39*, 1741-1771. DOI: 10.1016/S0014-3057(03)00100-9
- (5) Yates, C. R.; Hayes, W. Synthesis and applications of hyperbranched polymers. *Eur. Polym. J.*, **2004**, *40*, 1257-1281. DOI: 10.1016/j.eurpolymj.2004.02.007
- (6) Carlmark, A.; Hawker, C.; Hult, A.; Malkoch, M. New methodologies in the construction of dendritic materials. *Chem. Soc. Rev.*, **2009**, *38*, 352-362. DOI: 10.1039/b711745k
- (7) Wang, D.; Zhao, T.; Zhu, X.; Yan, D.; Wang, W. Bioapplications of hyperbranched polymers. *Chem. Soc. Rev.*, **2015**, *44*, 4023-4071. DOI: 10.1039/c4cs00229f

- (8) Zheng, Y.; Li, S.; Weng, Z.; Gao, C. Hyperbranched polymers: Advances from synthesis to applications. *Chem. Soc. Rev.*, **2015**, *44*, 4091-4130. DOI: 10.1039/c4cs00528g
- (9) Caminade, A.; Yan, D.; Smith, D. K. Dendrimers and hyperbranched polymers. *Chem. Soc. Rev.*, **2015**, *44*, 3870-3873. DOI: 10.1039/c5cs90049b
- (10) Cuneo, T.; Gao, H. Recent advances on synthesis and biomaterials applications of hyperbranched polymers. *Wiley Interdiscip. Rev. Nanomed. Nanobiotechnol.*, **2020**, *12*, e1640. DOI: 10.1002/wnan.1640
- (11) Kim, Y. H.; Webster, O. W. Hyperbranched polyphenylenes. *Polym. Prep.*, **1988**, *29*, 310-311
- (12) Kim, Y. H.; Webster, O. W. Hyperbranched polymers. *J. Macromolecules Sci.*, **2002**, *42*, 55-89. DOI: 10.1081/MC-120003095
- (13) Fréchet, J.; Henmi, M.; Gitsov, I.; Aoshima, S.; Leduc, M.; Grubbs, R. Self-condensing Vinyl Polymerization: An Approach to Dendritic Materials. *Science*, **1995**, *269*, 1080-1083. DOI: 10.1126/science.269.5227.1080
- (14) Cao, M.; Zhong, M. Chain-growth branching radical polymerization: an inibramer strategy. *Polym. Int.*, **2022**, *71*, 501-507. DOI: 10.1002/pi.6315
- (15) Wang, X.; Gao, H. Recent Progress on Hyperbranched Polymers Synthesized via Radical-Based Self-Condensing Vinyl Polymerization. *Polymers*, **2017**, *9*, 188. DOI: 10.3390/polym9060188
- (16) Shipp, D. A. Reversible-Deactivation Radical Polymerizations. *Polym. Rev.*, **2011**, *51*, 99-103. DOI: 10.1080/15583724.2011.566406
- (17) Corrigan, N.; Jung, K.; Moad, G.; Hawker, C. J.; Matyjaszewski, K.; Boyer, C. Reversible-deactivation radical polymerization (Controlled/living radical polymerization): From discovery

to materials design and applications. *Prog. Polym. Sci.*, **2020**, *111*, 101311-101333. DOI: 10.1016/j.progpolymsci.2020.101311

(18) Mori, H.; Müller, A.; Simon, P. Self-Condensing Vinyl Polymerization. *Hyperbranched Polymers: Synthesis, Properties, and Applications*, by Yan, Gao, and Frey, John Wiley & Sons, Inc. 139-174.

(19) Tsarevsky, N. V.; Matyjaszewski, K. “Green” Atom Transfer Radical Polymerization: From Process Design to Preparation of Well-Defined Environmentally Friendly Polymeric Materials. *Chem. Rev.*, **2007**, *107*, 2270-2299. DOI: 10.1021/cr050947

(20) Hawker, C. J.; Fréchet, J.; Grubbs, R.; Dao, J. Preparation of Hyperbranched and Star Polymers by a “Living”, Self-Condensing Free Radical Polymerization. *J. Am. Chem. Soc.*, **1995**, *117*, 10763-10764. DOI: 10.1021/ja00148a027

(21) Alfurhood, J. A.; Bachler, P. R.; Sumerlin, B. S. Hyperbranched polymers via RAFT self-condensing vinyl polymerization. *Polym. Chem.*, **2016**, *7*, 3361-3369. DOI: 10.1039/c6py00571c

(22) Zhuang, Y.; Deng, H.; Su, Y.; He, L. H.; Wang, R.; Tong, G. T.; He, D.; Zhu, X. Aptamer-Functionalized and Backbone Redox-Responsive Hyperbranched Polymer for Targeted Drug Delivery in Cancer Therapy. *Biomacromolecules*, **2016**, *17*, 2050-2062. DOI: 10.1021/acs.biomac.6b00262

(23) Vogt, A. P.; Gondi, S. R.; Sumerlin, B. S. Hyperbranched Polymers via RAFT Copolymerization of an Acryloyl Trithiocarbonate. *Aust. J. Chem.*, **2007**, *60*, 396-399. DOI: 10.1071/CH07077

- (24) Weng, Z.; Zheng, Y.; Tang, A.; Gao, C. Synthesis, Dye Encapsulation, and Highly Efficient Colouring Application of Amphiphilic Hyperbranched Polymers. *Aust. J. Chem.*, **2014**, *67*, 103-111. DOI: 10.1071/CH13353
- (25) Li, C.; Liu, H.; Tang, D.; Zhao Y. Synthesis, postmodification and fluorescence properties of reduction-cleavable core-couplable miktoarm stars with a branched core. *Polym. Chem.*, **2015**, *6*, 1474-1486. DOI: 10.1039/c4py01495b
- (26) Zheng, Y.; Tang, A.; Weng, Z.; Cai, S.; Jin, Y.; Gao, Z.; Gao, C. Amphiphilic Hyperbranched Polymers: Synthesis and Host-Guest Supramolecular Coloring Application. *Macromol. Chem. Phys.*, **2016**, *217*, 380-389. DOI: 10.1002/macp.201500321
- (27) Alfurhood, J. A.; Sun, H.; Bachler, P. R. Sumerlin, B. S. Hyperbranched poly(N-(2-hydroxypropyl) methacrylamide) via RAFT self-condensing vinyl polymerization. *Polym. Chem.*, **2016**, *7*, 2099-2104. DOI: 10.1039/C6PY00111D
- (28) Calvo, P. R.; Sparks, C. A.; Hochberg, J.; Wagener, K. B.; Sumerlin, B. S. Hyperbranched Bisphosphonate-Functional Polymers via Self-Condensing Vinyl Polymerization and Postpolymerization Multicomponent Reactions. *Macromol. Rapid Commun.*, **2021**, *42*, 2000578. DOI: 10.1002/marc.20200057
- (29) Zhang, C.; Zhou, Y.; Liu, Q.; Li, S.; Perrier, S.; Zhao, Y. Facile Synthesis of Hyperbranched and Star-Shaped Polymers by RAFT Polymerization Based on a Polymerizable Trithiocarbonate. *Macromolecules*, **2011**, *44*, 2034-2049. DOI: 10.1021/ma1024736
- (30) Carter, S.; Hunt, B.; Rimmer, S. Highly Branched Poly(N-isopropylacrylamide)s with Imidazole End Groups Prepared by Radical Polymerization in the Presence of a Styryl Monomer Containing a Dithioester Group. *Macromolecules*, **2005**, *38*, 4595-4603. DOI: 10.1021/ma047742n

- (31) Zhang, Y.; Teo, B. N.; Postma, A.; Ercole, F.; Ogaki, R.; Zhu, M.; Städler, B. Highly-Branched Poly(N-isopropylacrylamide) as a Component in Poly(dopamine) Films. *J. Phys. Chem. B*, **2013**, *117*, 10504-10512. DOI: 10.1021/jp407106z
- (32) Heidenreich, A. J.; Puskas, J. E. Synthesis of Arborescent (Dendritic) Polystyrenes via Controlled Inimer-Type Reversible Addition-Fragmentation Chain Transfer Polymerization. *J. Polym. Sci. Part: A Polym. Chem.*, **2008**, *46*, 7621-7627. DOI: 10.1002/pola.23062
- (33) Ishizu, K.; Mori, A. Synthesis of hyperbranched polymers by self-addition free radical vinyl polymerization of photo functional styrene. *Macromol. Rapid Commun.*, **2000**, *21*, 665-668. DOI: 10.1002/1521-3927(20000601)21:10<665::AID-MARC665>3.0.CO;2-M
- (34) Wang, Z.; He, J.; Tao, Y.; Yang, L.; Jiang, H.; Yang, Y. Controlled Chain Branching by RAFT-Based Radical Polymerization. *Macromolecules*, **2003**, *36*, 7446-7452. DOI: 10.1021/ma025673b
- (35) Zhang, M.; Liu, H.; Shao, W.; Miao, K.; Zhao, Y. Synthesis and Properties of Multicleavable Amphiphilic Dendritic Comblike and Toothbrushlike Copolymers Comprising Alternating PEG and PCL Grafts. *Macromolecules*, **2013**, *46*, 1325-1336. DOI: 10.1021/ma3025283
- (36) Wei, Z.; Hao, X.; Kambouris, P. A.; Gan, Z.; Hughes, T. C. One-pot synthesis of hyperbranched polymers using small molecule and macro RAFT inimers. *Polymer*, **2012**, *53*, 1429-1436. DOI: 10.1016/j.polymer.2012.02.011
- (37) Hu, X.; Liu, G.; Li, Y.; Wang, X.; Liu, S. Cell-Penetrating Hyperbranched Polyprodrug Amphiphiles for Synergistic Reductive Milieu-Triggered Drug Release and Enhanced Magnetic Resonance Signals. *J. Am. Chem. Soc.*, **2015**, *137*, 362-368. DOI: 10.1021/ja5105848

- (38) Tang, T.; Guo, W.; Xu, Y.; Xu, D. Synthesis and characterization of novel hyperbranched fluorescent polymers that can be precisely used for metal ion detection and quantification. *J. Appl. Polym. Sci.*, **2020**, *137*, 48933-48942. DOI: 10.1002/APP.48933
- (39) Wei, Z.; Hao, X.; Gan, Z.; Hughes, T. C. One-Pot Synthesis of Hyperbranched Glycopolymers by RAFT Polymerization. *J. Polym. Sci. Part A: Polym. Chem.*, **2012**, *50*, 2378-2388. DOI: 10.1002/pola.26012
- (40) Li, S.; Han, J.; Gao, C. High-density and hetero-functional group engineering of segmented hyperbranched polymers via click chemistry. *Polym. Chem.*, **2013**, *4*, 1774-1787. DOI: 10.1039/c2py20951a
- (41) Rahemipour, S.; Kohestanian, M.; Pourjavadi, A.; Vazifehkhori, H. H.; Mehrali, M. Synthesis and Properties of Multi-stimuli-Responsive Water-Soluble Hyperbranched Polymers Prepared Via Reversible Addition–Fragmentation Chain Transfer Self-Condensing Vinyl Polymerization. *ACS Appl. Polym. Mater.*, **2022**, *4*, 692–702. DOI: 10.1021/acsapm.1c01608
- (42) Kohestanian, M.; Keshavarzi, N.; Pourjavadi, A.; Rahmani, F. Fabrication of pH and thermal dual-responsive hyperbranched copolymer grafted magnetic graphene oxide via surface-initiated RAFT-SCVP for controlled release of DOX. *Materials Today Com.*, **2023**, *35*, 105504-105515. DOI: 10.1016/j.mtcomm.2023.105504
- (43) Wang, K.; Peng, H.; Thurecht, K. J.; Puttick, S.; Whittaker, A. K. Segmented Highly Branched Copolymers: Rationally Designed Macromolecules for Improved and Tunable 19F MRI. *Biomacromolecules*, **2015**, *16*, 2827-2839. DOI: 10.1021/acs.biomac.5b00800
- (44) Ferji, K.; Venturini, P.; Cleymand, F.; Chassenieux, C.; Six, J. In situ Glyco-nanostructures Formulation via Photo-Polymerization Induced Self-Assembly. *Polym. Chem.*, **2018**, *9*, 2868-2872. DOI: 10.1039/C8PY00346G (SI)

(45) Min, K.; Gao, H. New Method to Access Hyperbranched Polymers with Uniform Structure via One-Pot Polymerization of Inimer in Microemulsion. *J. Am. Chem. Soc.*, **2012**, *134*, 15680–15683. DOI: 10.1021/ja307174h

(46) Graff, R. W.; Wang, X. Gao, H. Exploring Self-Condensing Vinyl Polymerization of Inimers in Microemulsion To Regulate the Structures of Hyperbranched Polymers. *Macromolecules*, **2015**, *48*, 2118-2126. DOI: 10.1021/acs.macromol.5b00278

(47) Li, S. J.; Xie, S. J.; Li, Y. C.; Qian, H. J.; Lu, Z. Y. Influence of molecular-weight polydispersity on the glass transition of polymers. *Phys. Rev. E*, **2016**, *93*, 012613. DOI: 10.1103/PhysRevE.93.012613

(48) Simon, P.; Müller, E. Synthesis of Hyperbranched and Highly Branched Methacrylates by Self-Condensing Group Transfer Copolymerization. *Macromolecules*, **2001**, *34*, 6206-6213. DOI: 10.1021/ma002156p

ACKNOWLEDGMENTS

The authors thank the Agence Nationale de la Recherche (PRC 21-CE06-0001-01 – HBP-MultiReact) for financial support. The authors would also like to thank Sullivan Bricaud for NMR experiments and Alexandre Bénard, Kexin Zhang and Mireille Barthe for SEC experiments.

ASSOCIATED CONTENT

Precisions on experimental conditions for RAFT-SCVP, R-transmer conversion and MMA conversion calculated by ^1H NMR spectroscopy, Mark-Houwink-Sakurada plot for the purified HBP-R, 2D NMR spectra for purified HBP-R, DB determinations by inverse-gated decoupled ^{13}C NMR spectroscopy and ^1H NMR spectroscopy, MMA/R-transmer molar ratios determined by ^1H NMR spectroscopy.

AUTHOR INFORMATION

Corresponding Authors

*E-mail: Sagrario.pascual@univ-lemans.fr

Author Contributions

The manuscript was written through contributions of all authors. All authors have given approval to the final version of the manuscript.